Supporting Information:

One-pot In-situ Construction of Amine and Hydroxyl Co-modified Layered Double Hydroxides via Hydrothermal Method for Selective Scandium Adsorption

Siyu Huang,[a,b] Cheng-Zong Yuan,[a,b]* Jiang Li,[a,b] Lunliang Zhang,[a,b] Hongrui Zhao,[a,b] Wenkai Zhao,[a,b] Xiaomeng Zhang,[a,b,c,d]*

[a.] Institute of Resources and Ecological Environment, Jiangxi Province Key Laboratory of Cleaner Production of Rare Earths, Ganjiang Innovation Academy, Chinese Academy of Science, Ganzhou 341119, China;

[b.] School of Rare Earth, University of Science and Technology of China, Hefei, 230026, China;

[c.] State Key Laboratory of Multiphase Complex Systems, Institute of Process Engineering, Chinese Academy of Science, Beijing 100190, China;

[d.] Institute of Green Process Manufacturing Innovation, Chinese Academy of Science, Beijing 100190, China;

* Corresponding author (Email: czyuan@mail.ustc.edu.cn, xmzhang@gia.cas.cn.)

1. Methods

The adsorption capacity(Q_e), distribution coefficients(K_d) and separation coefficients (SF) were calculated by Eq.1,[2] Eq.2[3] and Eq.3 respectively.

$$Q_e = \frac{(C_0 - C_e)V}{m} \quad \textbf{(1)}$$

$$K_d = \frac{Q}{C_e} \quad \textbf{(2)}$$

$$SF_{A/B} = \frac{K_{dA}}{K_{dB}} \quad \textbf{(3)}$$

Where C_0 (mg/L) and C_e (mg/L) are the initial and equilibrium concentrations of metal ions, respectively, V(mL) is the volume of the initial metal ion solution, and m (mg) is the mass of the adsorbent.

For deeply explore the kinetic characteristics of scandium adsorption by LDHs and KH550-LDHs, the influence of time on adsorption capacity was studied and the results were shown in the Fig. S5. All materials basically reach equilibrium within 4 h tested at pH 5. Two kinetic models (pseudo-first-order Eq.1 and pseudo-second-order model Eq.2) were frequently applied to fit the data and its results are shown in **Table S3**. The linearization of kinetic model was performed by comparing the correlation coefficient R2 values. To further elucidate the diffusion mechanism of scandium on adsorbents, an intra particle diffusion model (Eq.3)[4] was used to fit the experimental data, and the results are shown in the **Table S4**.

$$q_t = q_e - q_e e^{-k1t} \quad \textbf{(1)}$$

$$q_t = \frac{k_2 q_e^2 t}{1 + k_2 q_e t} \quad \textbf{(2)}$$

$$q_t = k_3 \bullet t^{1/2} + C \quad \textbf{(3)}$$

In the equations, q_t and q_e are the adsorption capacity of adsorbent to adsorbate at time t and equilibrium state respectively (mg/g); k_1, k_2 and k_3 represent pseudo-first-order adsorption rate constant (g/(mg·min)), pseudo-second-order adsorption rate constant (g/(mg·min))and intraparticle diffusion rate constant (g/(mg·$min^{1/2}$)) respectively. C is the constant value related to thickness and boundary layer Number.

It were studied that the adsorption isotherms between pure LDHs and KH550-LDHs to further explore the relationship between adsorbent and adsorbate. For describe the Sc^{3+} adsorption behavior on materials, three classical adsorption models, namely, the Langmuir (Eq.4), and Freundlich (Eq.5),[5] were used to the measured data. The maximum adsorption capacity for KH550-LDHs and pure LDHs was calculated from sorption isotherm experiments at pH 5. It is attributed to the effective modification of KH550. The Langmuir and Freundlich models are used to fit the experimental data in **Fig. S6**, and the obtained parameters and correlation coefficients (R^2) values are listed in **Table S5**.

$$q_e = \frac{K_L q_m C_e}{1 + K_L C_e} \quad \textbf{(4)}$$

$$q_e = K_F C_e^{1/n} \quad \textbf{(5)}$$

$$R\ddot{N}H_2 + Sc^{3+} \rightleftharpoons Sc(RNH_2)^{3+} \quad \textbf{(6)}$$

$$3RNH_3{}^+ \bullet NO_3{}^- + Sc(NO_3)_6{}^{3-} \rightleftharpoons (RNH_3{}^+)_3 Sc(NO_3{}^-)_6 + 3NO_3{}^- \quad \textbf{(7)}$$

Where q_e and C_e represent equilibrium adsorption capacity (mg/g) and adsorption concentration (mg/L) respectively; q_m is adsorbance quantity (mg/g); K_L and K_F represent the empirical constants of the Langmuir and Freundlich model respectively; n is characteristic constant of adsorption strength.

2. Figures and tables

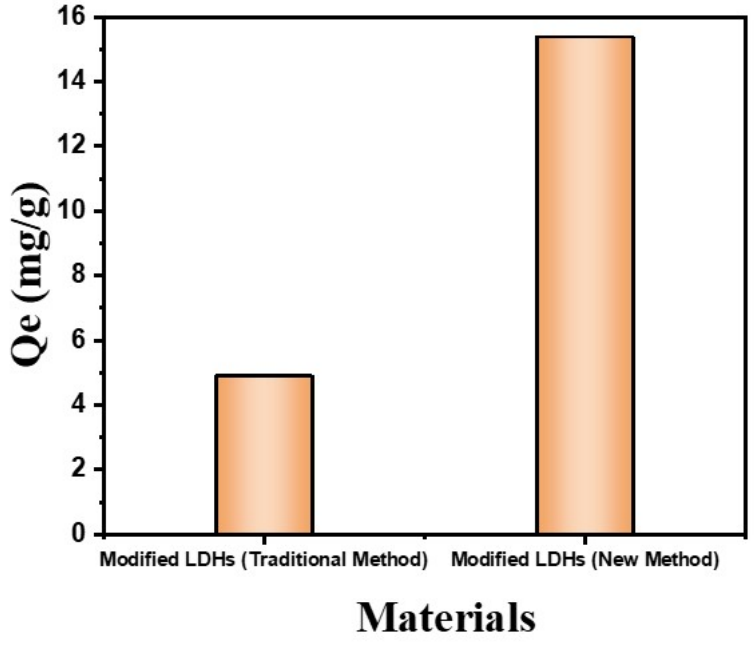

Fig.S1 Comparison of the adsorption effects of new and old modification methods on Sc^{3+}

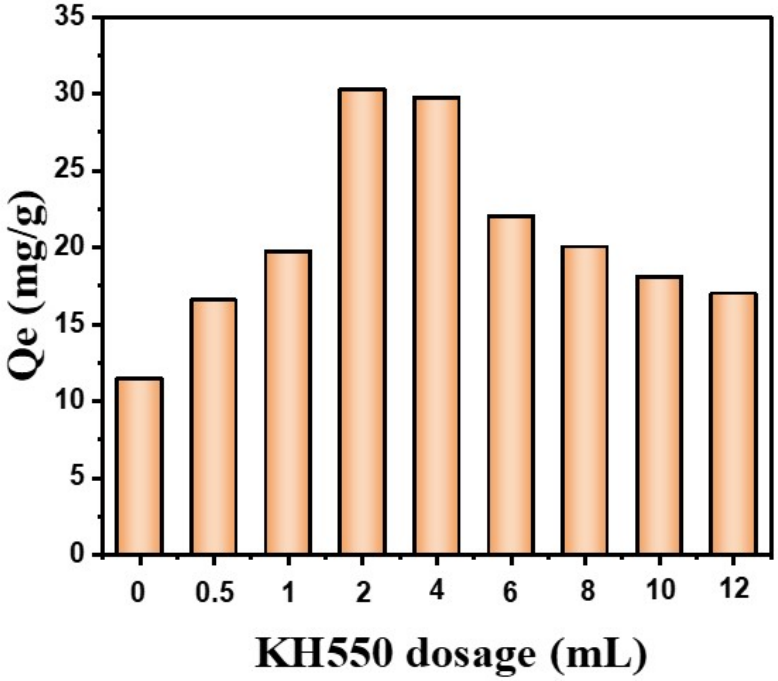

Fig.S2 The effect of volume of KH550 on the absorption ability of KH550-LDHs

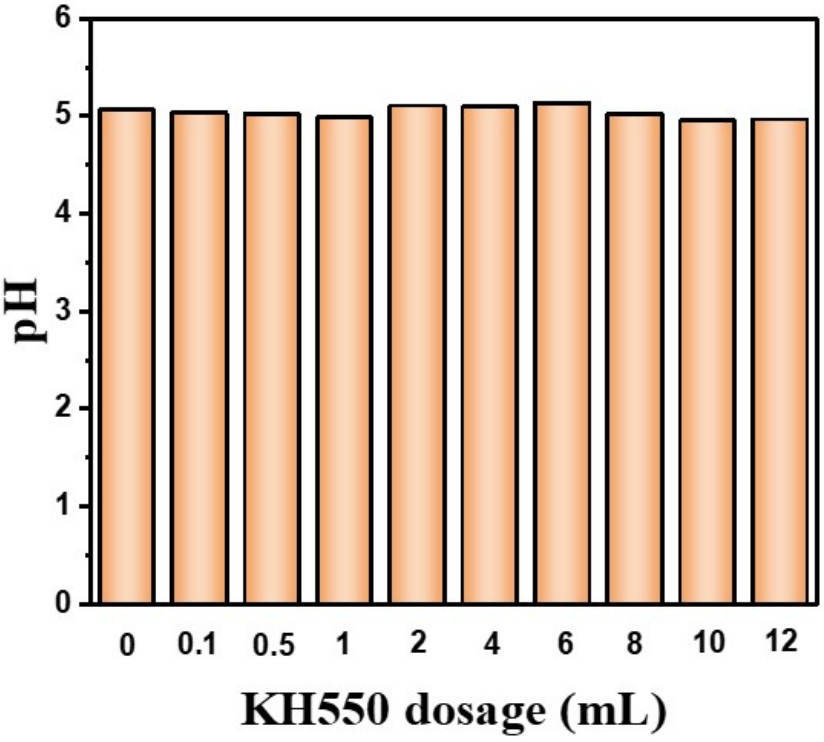

Fig.S3 pH of solution after adsorption (initial pH = 5.00±0.01)

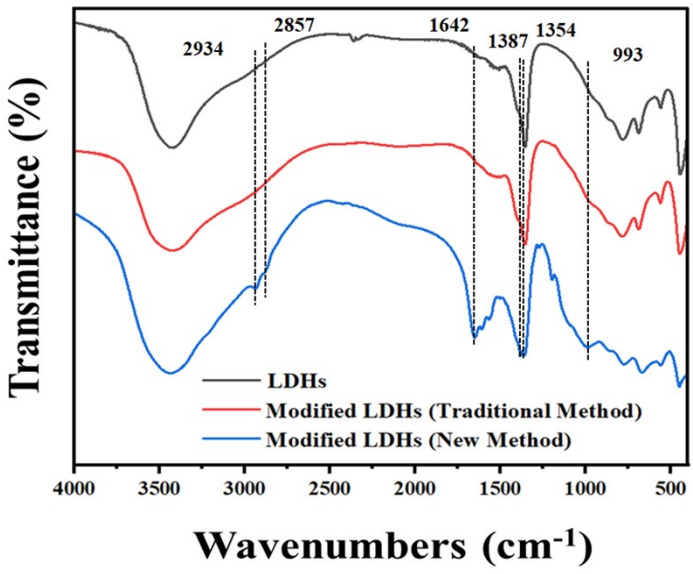

Fig.S4 Comparison of infrared spectra between traditional and new modified methods

Table S1. Dissolution concentration of material elements

Sample	Mg (ppm)	Al (ppm)	Si (ppm)
LDHs	2.113	2.56	0.4881
1K-LDHs	5.175	4.833	1.053
2K-LDHs	7.023	6.777	1.303
4K-LDHs	7.229	5.155	2.745
6K-LDHs	4.954	3.853	3.383

Table S2. N_2 adsorption parameters of LDHs and KH550-LDHs.

Samples	**BET surface area (m^2 /g)**	**Pore volume (cm^3 /g)**	**Pore size (nm)**
LDHs	41.2920	0.085100	8.2438
1K-LDHs	94.4019	0.163934	6.9315
2K-LDHs	87.9409	0.215982	9.9928
4K-LDHs	43.7906	0.170775	15.5993
6K-LDHs	4.9630	0.022093	17.8060

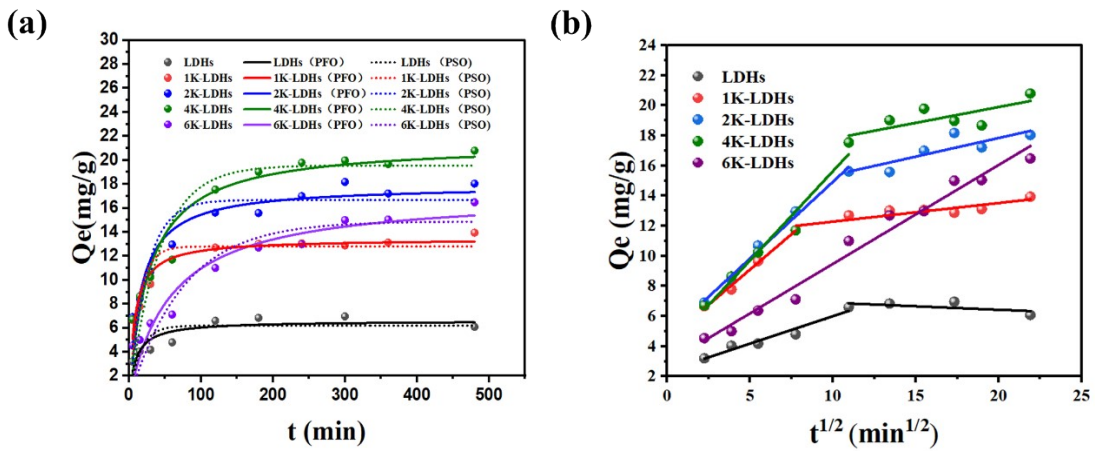

Fig. S5 The fitting of pseudo-first and second order (a), and Intra-particle diffusion model (d) for adsorption of Sc^{3+}onto KH550-LDHs.

Table S3. Fitting parameters of adsorption kinetics using pseudo-first and second order models.

Samples	Pseudo-first order			Pseudo-second order		
	K_1 (min^{-1})	Qe ($mg\ g^{-1}$)	R^2	K_2 ($g\ mg^{-1}\ min^{-1}$)	Qe ($mg\ g^{-1}$)	R^2
LDHs	0.0650	6.196	0.5774	0.0164	6.5900	0.7734
1K-LDHs	0.0716	12.797	0.7662	0.0092	13.4241	0.9178
2K-LDHs	0.0407	16.670	0.8147	0.0026	17.9076	0.9204
4K-LDHs	0.0239	19.550	0.8464	0.0017	21.4496	0.9112
6K-LDHs	0.0407	16.670	0.8147	0.0010	17.2074	0.9001

Table S4. Kinetic parameters calculated from Weber-Morris model for Sc^{3+} adsorption onto KH550-LDHs.

Sample	First stage		Second stage	
	K_1	R^2	K_2	R^2
LDHs	0.364	0.976	-0.0467	0.3285
1K-LDHs	0.938	0.996	0.1248	0.9020
2K-LDHs	1.019	0.996	0.8587	0.247
4K-LDHs	1.185	0.982	0.2101	0.757
6K-LDHs	0.657	0.989	0.657	0.989

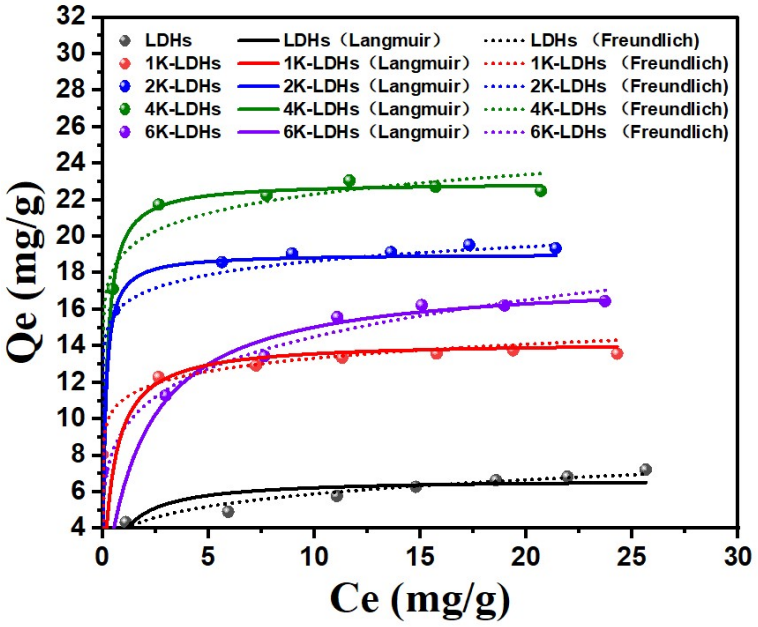

Fig. S6 Extraction isotherms of Sc for adsorption Sc^{3+} onto KH550-LDHs.

Table S5. Fitting parameters of adsorption isotherm using Langmuir, Freundlich and Temkin models.

Sample	Freundlich			Langmuir		
	K_F	n	R_F^2	Q_m	b	R_L^2
LDHs	3.104	3.858	0.998	6.713	1.289	0.680
1K-LDHs	11.172	13.055	0.716	13.810	2.908	0.923
2K-LDHs	16.302	19.305	0.862	19.362	8.252	0.972
4K-LDHs	18.871	13.663	0.842	22.963	6.080	0.982
6K-LDHs	9.252	0.837	0.943	17.809	0.541	0.947

Table S6. Comparison of adsorption properties for Sc with other adsorbents.

Sorbent	pH	Q_{max}(mg/g)	Reference
Mesoporous Silica	3	1.00	[3]
GA-g-PAM/SiO_2 nanocomposite	6	11.05	[6]
750°C calcinated H_3PO_4 activated biochar	3	20.77	[7]
Ionic liquid-Amberlite	3	16.18	[8]
Nano modified AC	2	10.11	[9]
PAN grafted SWNT-APTES nano-silica	4	12.68	[10]
LDHs	5	7.599	This paper
4K-LDHs	5	22.73	This paper

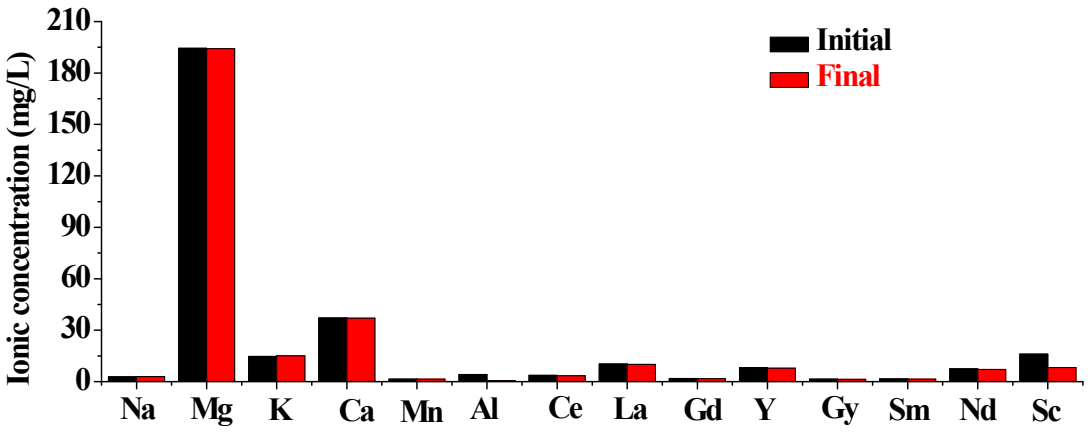

Fig. S7 The adsorption experiment under realistic environmental conditions. In this experiments, the RE solution was taken from Sanqiu Mine, and we have added the Sc ion to evaluate the performances of 4k-LDHs.

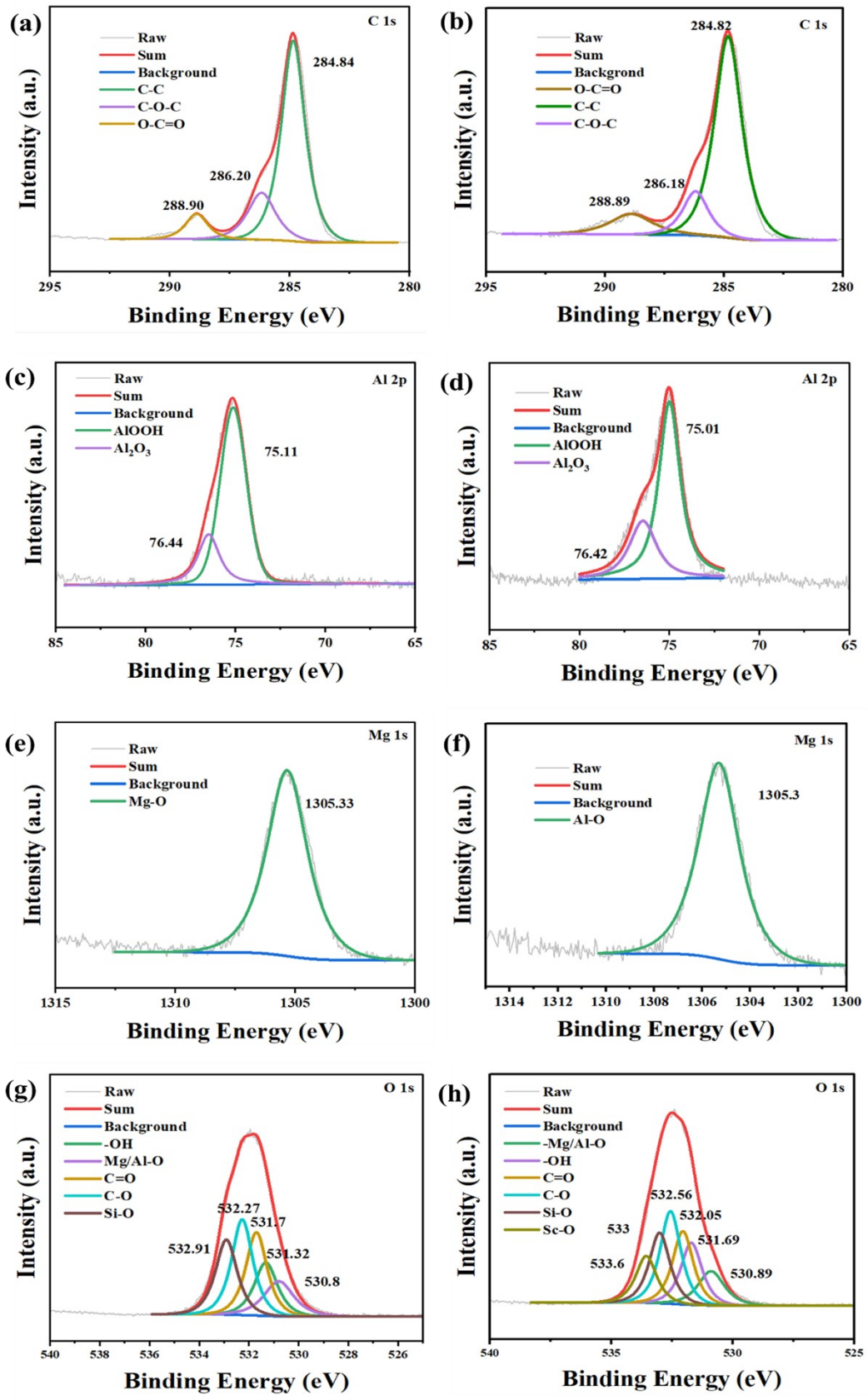

Fig. S8 The XPS spectra of individual element of modified LDH before and after adsorption.

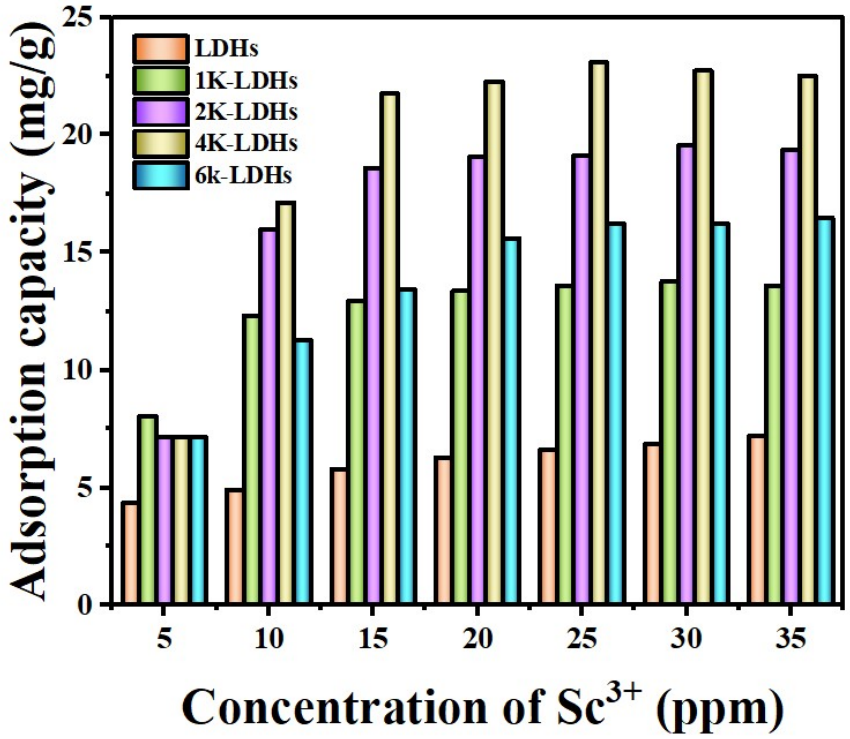

Fig. S9 Effect of different adsorbents addition levels on Sc^{3+} concentration.

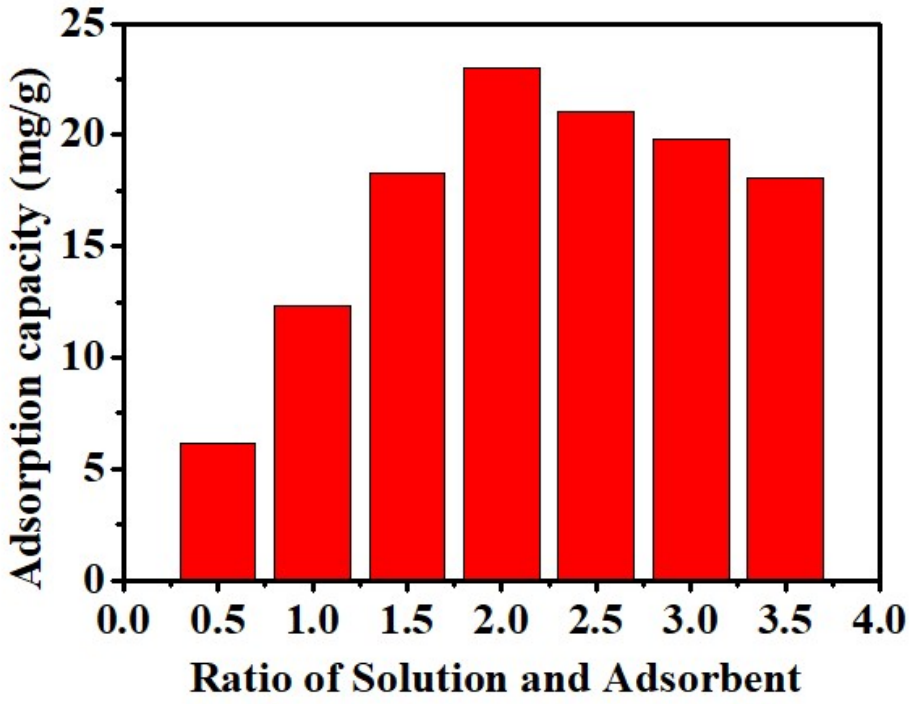

Fig. S10 The adsorption performances for different adsorbent loading of the synthesized material. Specifically, when 10 mg adsorbent and 20 mL of a Sc^{3+} solution were selected, the adsorption capacity of synthesized material reached 22.73 mg/g.

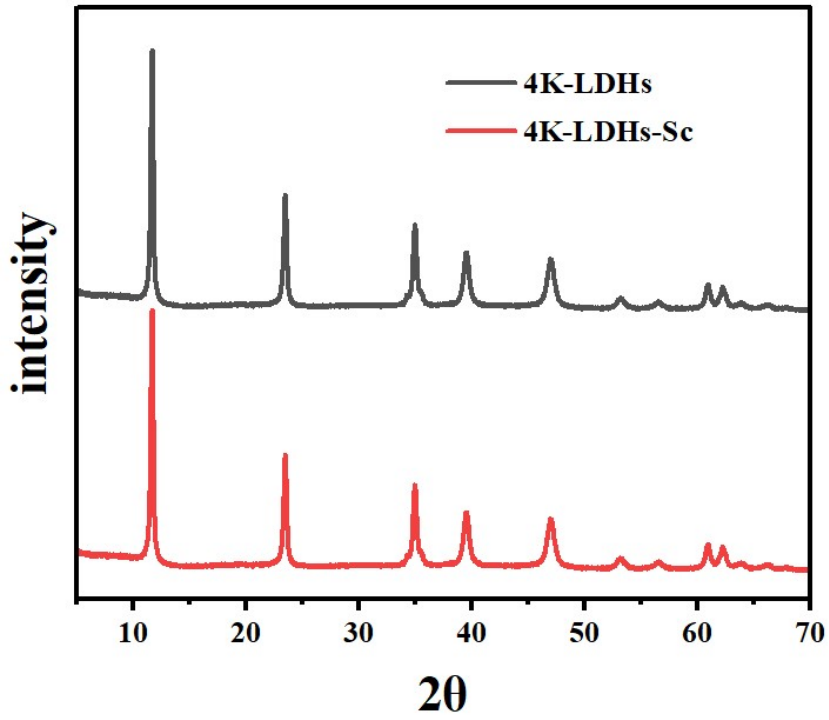

Fig. S11 XRD patterns of before and after material adsorption of scandium.

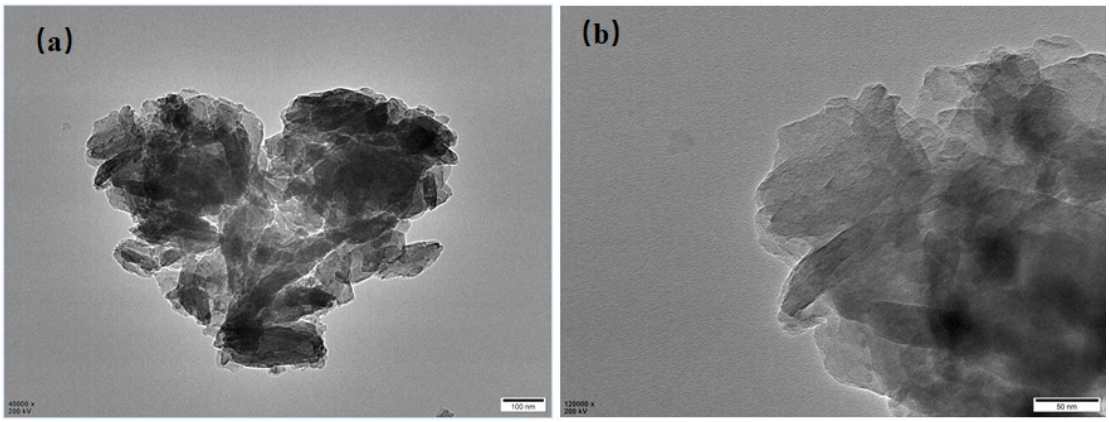

Fig. S12 The TEM analysis of adsorbent after Sc^{3+} adsorption.

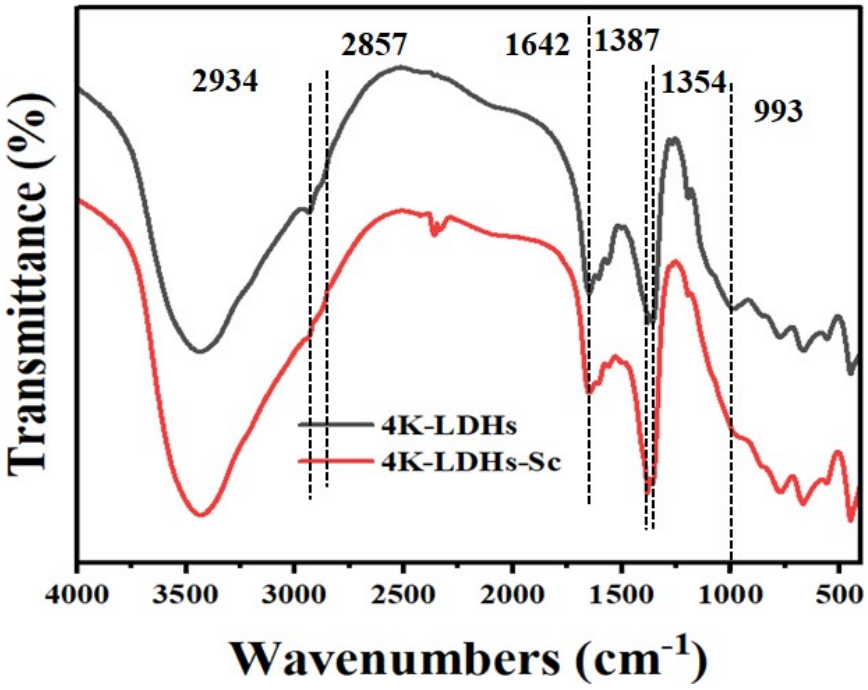

Fig. S13 Comparison of infrared spectra before and after material adsorption of scandium.

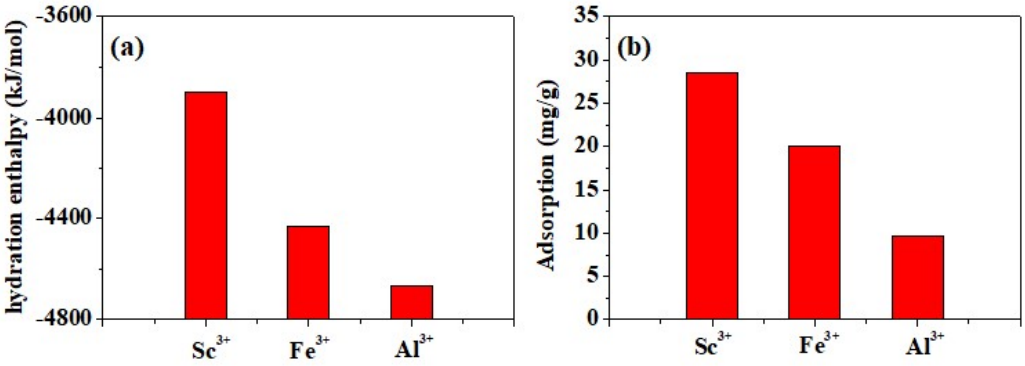

Figure S14 (a) The hydration enthalpy of Sc (-3897 kJ/mol), Fe (-4430 kJ/mol) and Al (-4665 kJ/mol). (b) The adsorption activity of 4k-LDHs for Sc^{3+}, Fe^{3+} and Al^{3+}.

References

1. P. C. Gu, S. Zhang, X. Li, X. X. Wang, T. Wen, R. Jehan, A. Alsaedi, T. Hayat and X. K. Wang, *Environ. Pollut.*, 2018, **240**, 493-505.
2. H. Mohammedi, H. Miloudi, A. Boos and C. Bertagnolli, *Environ. Sci Pollut. Res. Int.*, 2020, **27**, 26943-26953.
3. S. Giret, Y. Hu, N. Masoumifard, J. F. Boulanger, J. Estelle, F. Kleitz and D. Lariviere, *ACS Appl. Mater. Interfaces,* 2018, **10**, 448-457.
4. Q. Zhou, T. Luo, H. Yang, C. Liang, L. Jing and W. Luo, *J. Colloid Interface Sci.*,

2018, **513**, 427-437.
5. S. Iftekhar, V. Srivastava, D. L. Ramasamy, W. A. Naseer and M. Sillanpää, *Chem. Eng. J.,*, 2018, **347**, 398-406.
6. S. Iftekhar, V. Srivastava, A. Casas and M. Sillanpää, *J. Clean. Prod.,* 2018, **170**, 251-259.
7. X. Dai, N. Thi Hong Nhung, M. F. Hamza, Y. Guo, L. Chen, C. He, S. Ning, Y. Wei, G. Dodbiba and T. Fujita, *Sep. Purif. Technol.,* 2022, **292**.
8. D. Avdibegović, M. Regadío and K. Binnemans, *RSC Adv.*, 2017, **7**, 49664-49674.
9. I. V. Burakova, A. E. Burakov, A. G. Tkachev, I. D. Troshkina, O. A. Veselova, A. V. Babkin, W. M. Aung and I. Ali, *J. Mol. Liq.,* 2018, **253**, 277-283.
10. D. L. Ramasamy, V. Puhakka, B. Doshi, S. Iftekhar and M. Sillanpää, *Chem. Eng. J.,* 2019, **365**, 291-304.